ANNALS of Clinical and Translational Neurology
Open Access
AMERICAN NEUROLOGICAL ASSOCIATION

RESEARCH ARTICLE

Magnetization transfer ratio quantifies polyneuropathy in hereditary transthyretin amyloidosis

Jennifer Kollmer[1,2], Ute Hegenbart[2,3], Christoph Kimmich[2,3], Ernst Hund[2,4], Jan C. Purrucker[2,4], John M. Hayes[5], Stephen I. Lentz[6], Georges Sam[4], Johann M. E. Jende[1], Stefan O. Schönland[2,3], Martin Bendszus[1], Sabine Heiland[1,7] & Markus Weiler[2,4]

[1]Department of Neuroradiology, Heidelberg University Hospital, Heidelberg, Germany
[2]Amyloidosis Center Heidelberg, Heidelberg University Hospital, Heidelberg, Germany
[3]Medical Department V, Heidelberg University Hospital, Heidelberg, Germany
[4]Department of Neurology, Heidelberg University Hospital, Heidelberg, Germany
[5]Department of Neurology, University of Michigan, Ann Arbor, MI
[6]Department of Internal Medicine, Division of Metabolism, Endocrinology & Diabetes, University of Michigan, Ann Arbor, MI
[7]Division of Experimental Radiology, Department of Neuroradiology, Heidelberg University Hospital, Heidelberg, Germany

Correspondence
Jennifer Kollmer, Department of Neuroradiology, Heidelberg University Hospital, Im Neuenheimer Feld 400, D-69120 Heidelberg, Germany. Tel: +49 6221 567566; Fax: +49 6221 564673; E-mail: jennifer.kollmer@med.uni-heidelberg.de
or
Markus Weiler, Department of Neurology, Heidelberg University Hospital, Im Neuenheimer Feld 400, D-69120 Heidelberg, Germany. Tel: +49 6221 567504; Fax: +49 6221 565461; E-mail: markus.weiler@med.uni-heidelberg.de

Funding Information
The study was supported in part by Alnylam Pharmaceuticals (research grant to J.K.), the Medical Faculty of the University of Heidelberg (Olympia Morata stipend grant to J.K.), and the German Research Foundation (SFB 1118 to S.H., SFB 1158 to M.B.). S.H. was supported by the Dietmar Hopp Foundation, and M.B. by Siemens Healthcare, the Dietmar Hopp Foundation, and the European Union (Horizon 2020).

Received: 16 January 2020; Revised: 30 March 2020; Accepted: 31 March 2020

***Annals of Clinical and Translational Neurology* 2020; 7(5): 799–807**

doi: 10.1002/acn3.51049

Abstract

Objective: To quantify peripheral nerve lesions in symptomatic and asymptomatic hereditary transthyretin amyloidosis with polyneuropathy (ATTRv-PNP) by analyzing the magnetization transfer ratio (MTR) of the sciatic nerve, and to test its potential as a novel biomarker for macromolecular changes. **Methods**: Twenty-five patients with symptomatic ATTRv-PNP, 30 asymptomatic carriers of the mutant *transthyretin* gene (mut*TTR*), and 20 age-/sex-matched healthy controls prospectively underwent magnetization transfer contrast imaging at 3 Tesla. Two axial three-dimensional gradient echo sequences with and without an off-resonance saturation rapid frequency pulse were conducted at the right distal thigh. Sciatic nerve regions of interest were manually drawn on 10 consecutive axial slices in the images without off-resonance saturation, and then transferred to the corresponding slices that were generated by the sequence with the off-resonance saturation pulse. Subsequently, the MTR and cross-sectional area (CSA) of the sciatic nerve were evaluated. Detailed neurologic and electrophysiologic examinations were conducted in all ATTRv-PNP patients and mut*TTR*-carriers. **Results**: Sciatic nerve MTR and CSA reliably differentiated between ATTRv-PNP, mut*TTR*-carriers, and controls. MTR was lower in ATTRv-PNP (26.4 ± 0.7; $P < 0.0001$) and in mut*TTR*-carriers (32.6 ± 0.8; $P = 0.0005$) versus controls (39.4 ± 2.1), and was also lower in ATTRv-PNP versus mut*TTR*-carriers ($P = 0.0009$). MTR correlated negatively with the NIS-LL and positively with CMAPs and SNAPs. CSA was higher in ATTRv-PNP (34.3 ± 1.7 mm^3) versus mut*TTR*-carriers (26.0 ± 1.1 mm^3; $P = 0.0005$) and versus controls (20.4 ± 1.2 mm^3; $P < 0.0001$). CSA was also higher in mut*TTR*-carriers versus controls. **Interpretation**: MTR is a novel imaging marker that can quantify macromolecular changes in ATTRv-PNP and differentiate between symptomatic ATTRv-PNP and asymptomatic mut*TTR*-carriers and correlates with electrophysiology.

Introduction

Hereditary transthyretin (ATTRv) amyloidosis is a devastating systemic disease that leads to death in 10 years, on average, after symptom onset if left untreated.[1,2] One of the main manifestations in ATTRv amyloidosis is a rapidly progressive distal-symmetric, sensorimotor polyneuropathy (PNP). Novel disease-modifying therapies

such as the transthyretin (TTR) stabilizing drug tafamidis meglumine (Vyndaqel®),[3] the RNA interference therapeutic patisiran (Onpattro®),[4] and the antisense oligonucleotide inotersen (Tegsedi®)[5] have shown beneficial effects on disease progression and quality of life. However, early diagnosis and initiation of treatment may be important to prevent irreversible nerve and organ damage. Unfortunately, there are well-known limitations of traditional diagnostic methods that lead to the following two main problems: First, determining the disease onset in previously asymptomatic carriers of the mutant *transthyretin gene* (mut*TTR*) is challenging due to the preferential involvement of small nerve fibers at early disease stages, and second, monitoring a potential therapeutic response in severely affected patients holds difficulties due to extinct electrophysiologic potentials at advanced PNP stages.[6–10]

MR neurography (MRN) can overcome some of the aforementioned diagnostic limitations by directly visualizing peripheral nerve lesions.[11–21] The quantitative MRN parameters, proton spin density (ρ) and apparent T2 relaxation time ($T2_{app}$), have previously proven their feasibility to detect subclinical and early nerve lesions as well as to differentiate between neuropathic patients and controls or even between different disease severities in several neuropathies.[14–18] However, the changes in macromolecular structures that underlie alterations in ρ and $T2_{app}$ still need to be elucidated. Here, magnetization transfer contrast (MTC) imaging can assist by providing information on the concentration of protons bound to macromolecules (including their interaction with free water molecules) that, due to their short T2 relaxation time, cannot be measured directly by conventional MRI sequences.[22–25] In the peripheral nervous system (PNS), MTC imaging has been applied in patients with Charcot–Marie–Tooth disease, and results were promising in that the calculated magnetization transfer ratio (MTR) correlated well with the disease severity and was suggested as a new biomarker.[26]

In this study, we aim to use MTR as a diagnostic tool to quantify sciatic nerve lesions in symptomatic and asymptomatic ATTRv amyloidosis with PNP (ATTRv-PNP) in comparison with clinical and electrophysiologic measurements, and with healthy controls.

Methods

Study design, neurologic, and electrophysiologic assessments

This prospective case–control study was approved by the institutional ethics board (University of Heidelberg; S-398/2012), and all participants gave written informed consent.

Fifty-five participants with genetically confirmed mut*TTR* (31 males, 24 females, mean age 50.4 years, range 22–76), and 20 sex-matched healthy volunteers (11 males, 9 females) were enrolled from December 2013 to April 2019. Age-matching of controls was performed after subdividing the ATTRv group into asymptomatic mut*TTR*-carriers and symptomatic ATTRv-PNP as described in the results section. Patients with prior liver transplantation or treatment with disease-modifying drugs were excluded from the study. Additional exclusion criteria for all groups were age <18 years, pregnancy, any MRI contraindications, any risk factors for a competing non-ATTRv-related PNP such as diabetes mellitus, alcoholism or malignant diseases, and any other neurologic disorders such as multiple sclerosis (MS).

A detailed medical history was taken from all participants with mut*TTR*, and comprehensive neurologic examinations were performed including assessments for the Neuropathy Impairment Score in the Lower Limbs (NIS-LL; E.H.; J.P.; M.W.).[27] Nerve conduction studies (NCS) assessed distal motor latencies (DML), compound muscle action potentials (CMAP), and nerve conduction velocities (NCV) of the peroneal and tibial nerves. Sensory nerve action potentials (SNAP) and NCVs were measured for the sural nerve (G.S.; M.W.). Skin temperature was controlled at a minimum of 32°C. Based on individual neurologic and electrophysiologic findings, all participants with proven mut*TTR* were further classified into either clinically symptomatic patients or asymptomatic mut*TTR*-carriers as described in previous publications.[15,16] Briefly, a NIS-LL score of 0 and NCS with not more than one pathologic parameter were required for assignment to the group of asymptomatic mut*TTR*-carriers. In symptomatic ATTRv-PNP, PNP severity was further subclassified as either mild to moderate (NIS-LL $\leq$ 44) or severe (NIS-LL> 44).

MRN imaging protocol

All participants were examined feet first, in supine position in a 3.0 Tesla MR scanner (Magnetom TIM-TRIO, Siemens Healthineers, Erlangen, Germany), and a 15-channel Transmit-Receive knee-coil (INVIVO, Gainesville, FL, USA) was positioned at the right distal thigh. The thigh was chosen as previous studies showed a strong predominance of nerve lesions at this anatomical location not only in ATTRv-PNP but also in other PNPs.[15,17,18] Two axial three-dimensional, gradient echo sequences with and without an off-resonance saturation pulse (Gaussian envelop, duration = 9984 μsec, frequency offset = 1200 Hz) were carried out at the exact same slice position and with the following exact same sequence parameters:

Repetition time = 47 msec, echo time = 4.92 msec, field of view = 160 × 160 mm^2, matrix-size 256 × 256, band-width = 370 Hz/Px, 16 slices, slice thickness = 3.5 mm, voxel-size = 0.7 × 0.6 × 3.5 mm^3, flip angle = 7°, acquisition time = 3:43 min.

The total acquisition time for this protocol including survey scans was 7:36 min.

Image analysis

After pseudonymization, all generated images were analyzed in ImageJ (version 1.51j8; National Institutes of Health, Bethesda, Maryland, MD, USA) by manually delineating the sciatic nerve circumference as intraneural region of interest (ROI) approximately 1 cm proximal of the nerve bifurcation (J.K.). All ROIs were primarily drawn on axial slices generated by the sequence without off-resonance saturation. The exact same ROIs were then transferred to the corresponding slices that were generated by the sequence with off-resonance saturation by using the "synchronize windows" tool in ImageJ. Any possible inaccuracy of ROI positions between the two sequences, for example, due to patient motion between the acquisition of the two sequences, was ruled out by visual inspection of each ROI. To avoid any artifacts or systematic errors caused by inhomogeneities of the B1-field of the saturation pulse, only the 10 central slices within each image slab were used for all analyses. The additional time needed for the post-processing including drawing of the ROIs and performing all necessary calculations was approximately 30 min per participant.

Magnetization transfer ratio

The MTR was calculated separately for each participant, and each evaluated axial imaging slice according to the following equation, in which S_0 is the signal without and S_1 with off-resonance saturation:

$$\mathrm{MTR} = 100 \times \frac{(S_0 - S_1)}{S_0}$$

MTR values were subsequently extracted from each slice position and averaged over all ten slice positions for each participant. Calculated MTR mean values of the sciatic nerve were then compared between the different groups (symptomatic ATTRv-PNP vs. asymptomatic mut*TTR*-carriers vs. controls).

Cross sectional area

Morphometric quantification was additionally performed by measuring the cross-sectional area (CSA) of the sciatic nerve per participant and per slice position. Subsequently, CSAs were averaged over all 10 slice positions per participant, and then compared between the three groups.

Statistical analyses

Statistical data analyses were performed with GraphPad Prism 7.03 (J.K.; J.M.H.). Differences in MTR and CSA between manifest ATTRv-PNP, asymptomatic mut*TTR*-carriers, and healthy controls were evaluated with a one-way ANOVA for a priori assumptions. Subsequent post hoc analyses were corrected for multiple comparisons by using the Tukey–Kramer test. The Mann–Whitney test was used to evaluate differences in the underlying mutation and in electrophysiologic test results between manifest ATTRv-PNP, and asymptomatic mut*TTR*-carriers. Pearson's correlation coefficients were calculated for additional correlation analyses between results from NCS and MTR/ CSA data. Additional data simulation and visualization of the MTR was performed using qMTLab within MatLab 9.6 (J.K.; J.M.H.; S.I.L.).[28]

Statistical tests were two-tailed and an alpha level of significance was defined at $P < 0.05$. All results are documented as mean values ± SEM.

Results

Clinical and electrophysiologic data

The Table summarizes mean values ± SEM as well as the corresponding range of important clinical and electrophysiologic data. Based on clinical and electrophysiologic examination results, 30 participants of the ATTRv-PNP group were classified as asymptomatic mut*TTR*-carriers (13 males, 17 females, mean age 43.3 years, range 22–62), while 25 participants were identified as symptomatic ATTRv-PNP patients (18 males, 7 females, mean age 58.8 years, range 33–76). The age of our control group (mean age 44.3 years, range 22–73) was matched with the age of asymptomatic mut*TTR*-carriers. In accordance with our classification criteria, all asymptomatic mut*TTR*-carriers scored "0" in the NIS-LL. Symptomatic ATTRv-PNP patients presented with moderate to severe clinical symptoms and abnormalities in sensory and motor function tests (e.g., numbness, painful paresthesia, loss of temperature sensation, and weakness). The mean NIS-LL in this group was 27.9 ± 4.3 (range 3–61.5; Table 1). Symptomatic patients additionally suffered from wide-spread amyloid-related systemic manifestations, for example, cardiac, gastrointestinal, and autonomic dysfunction, or carpal tunnel syndrome. Val30Met was the most prevalent point mutation found in 14 out of 25 asymptomatic mut*TTR*-carriers (56%) and in 15 out of 30 patients with symptomatic ATTRv-PNP (50%). Other mutations in our

Table 1. Summary of clinical and electrophysiologic data.

Parameter	Symptomatic ATTRv-PNP	Asymptomatic mut*TTR*-carriers	*P* value
NIS-LL score [0–88]	27.9 ± 4.3	0	<0.0001
Peroneal nerve DML [msec]	5.3 ± 0.4	3.6 ± 0.1	<0.0001
Peroneal nerve CMAP [mV]	2.0 ± 0.6	8.8 ± 0.7	<0.0001
Peroneal nerve NCV [m/sec]	40.6 ± 2.2	50.6 ± 0.8	0.0002
Tibial nerve DML [msec]	4.7 ± 0.3	3.4 ± 0.1	0.0004
Tibial nerve CMAP [mV]	3.6 ± 1.1	19.3 ± 1.4	<0.0001
Tibial nerve NCV [m/sec]	42.1 ± 1.8	51.4 ± 0.7	<0.0001
Sural nerve SNAP [μV]	3.6 ± 1.6	15.2 ± 1.2	<0.0001
Sural nerve NCV [m/sec]	45.6 ± 2.9	55.5 ± 1.4	0.0040

All results are presented as mean values ± SEM.
CMAP, compound muscle action potential; DML, distal motor latency; NCV, nerve conduction velocity; NIS-LL, Neuropathy Impairment Score in the Lower Limbs; SNAP, sensory nerve action potential.

cohort were Ile107Val (8x), Cys10Arg (4x), Leu58His (4x), Phe33Leu (3x) Ile84Asn (2x), Ala45Thr (2x), Val20Ile (2x), Val122Ile (1x), Glu54Gly (1x), Ile84Thr (1x), Ser50Arg (1x), Thr106Asn (1x). NCS revealed normal results of peroneal and tibial DMLs, CMAPs, and NCVs, as well as of sural SNAPs and NCVs in all asymptomatic mut*TTR*-carriers. In the symptomatic group, NCS confirmed the clinical findings of a PNP (i.e., NIS-LL score > 0) in 22 out of 25 patients by pathologic NCS findings, indicating either sensory, motor, or combined sensorimotor peripheral nerve lesions. The three patients with normal NCS findings in this group were classified as clinically symptomatic solely based on clearly pathologic NIS-LL scores (5, 9, and 15). Mean values of all analyzed NCS parameters are given in Table 1.

Magnetization transfer ratio

Sciatic nerve MTR was markedly different between the three groups (symptomatic ATTRv-PNP, asymptomatic mut*TTR*-carriers, healthy controls; one-way ANOVA $P < 0.0001$, *f*-value = 25.86). Mean MTR in healthy controls was 39.4 ± 2.1% (median: 36.5%) and decreased in asymptomatic mut*TTR*-carriers (32.6 ± 0.8%, $P = 0.0005$; median: 31.1%) and further decreased in symptomatic ATTRv-PNP patients (26.4 ± 0.7%, $P < 0.0001$; median: 25.3%). Differences between asymptomatic mut*TTR*-carriers and symptomatic ATTRv-PNP were also distinct ($P = 0.0009$) (Figs. 1A and 2). After subdividing the symptomatic ATTRv-PNP group into either mildly/moderately or severely affected patients, additional post hoc comparisons revealed that sciatic nerve MTR was lower in mild/moderate ATTRv-PNP (27.4 ± 0.9) versus asymptomatic mut*TTR*-carriers ($P = 0.0368$) and versus controls ($P < 0.0001$), while differences between mild/moderate and severe ATTRv-PNP were not observed ($P = 0.71$).

However, further correlation analyses with clinical and electrophysiologic parameters revealed a negative correlation between sciatic nerve MTR and the NIS-LL score ($r = -0.499$, $P = 0.0132$). In manifest ATTRv-PNP, sciatic nerve MTR positively correlated with peroneal ($r = 0.595$, $P = 0.0017$) and tibial CMAP amplitudes ($r = 0.418$, $P = 0.0241$) as well as with sural SNAP amplitudes ($r = 0.441$, $P = 0.0275$). No correlation was found between the sciatic nerve MTR and peroneal and tibial nerve DMLs, or peroneal, tibial, and sural NCVs in this group. In asymptomatic mut*TTR*-carriers a positive correlation was found between sciatic nerve MTR and sural SNAP amplitudes only ($r = 0.418$, $P = 0.0241$), while peroneal and tibial DMLs, CMAP amplitudes, and NCVs, as well as sural NCVs did not correlate.

Cross-sectional area

Mean CSA of the sciatic nerve was highly different between the three groups (one-way ANOVA $P < 0.0001$, *f*-value = 22.92). Post hoc comparisons showed a larger CSA in symptomatic ATTRv-PNP (34.3 ± 1.7 mm^2; median: 34.1 mm^2) than in controls (20.4 ± 1.2 mm^2, $P < 0.0001$; median: 18.2 mm^2) and also in asymptomatic mut*TTR*-carriers (26.0 ± 1.1 mm^2; median: 26.3 mm^2) compared to controls ($P = 0.0180$). Marked differences in sciatic nerve CSA between symptomatic and asymptomatic ATTRv-PNP participants were also observed ($P = 0.0001$; Figs. 1B and 2). Subgroup analyses for different clinical severities revealed higher sciatic nerve CSA in mildly/moderately affected ATTRv-PNP patients (32.1 ± 2.2 mm^2) compared to mut*TTR*-carriers ($P = 0.0263$) and compared to controls ($P < 0.0001$), while differences between mild/moderate and severe ATTRv-PNP were not significant ($P = 0.17$).

Sciatic nerve CSA inversely correlated with peroneal NCV (ATTRv-PNP: $r = -0.571$, $P = 0.0329$; mut*TTR*-carriers: $r = -0.386$, $P = 0.0387$) and tibial NCV (ATTRv-PNP: $r = -0.526$, $P = 0.0365$; mut*TTR*-carriers: $r = -0.394$, $P = 0.0343$). A positive correlation between sciatic nerve CSA and tibial nerve DMLs ($r = 0.498$, $P = 0.0498$), as well as a negative correlation with sural nerve SNAP amplitudes ($r = -0.399$, $P = 0.0476$) was

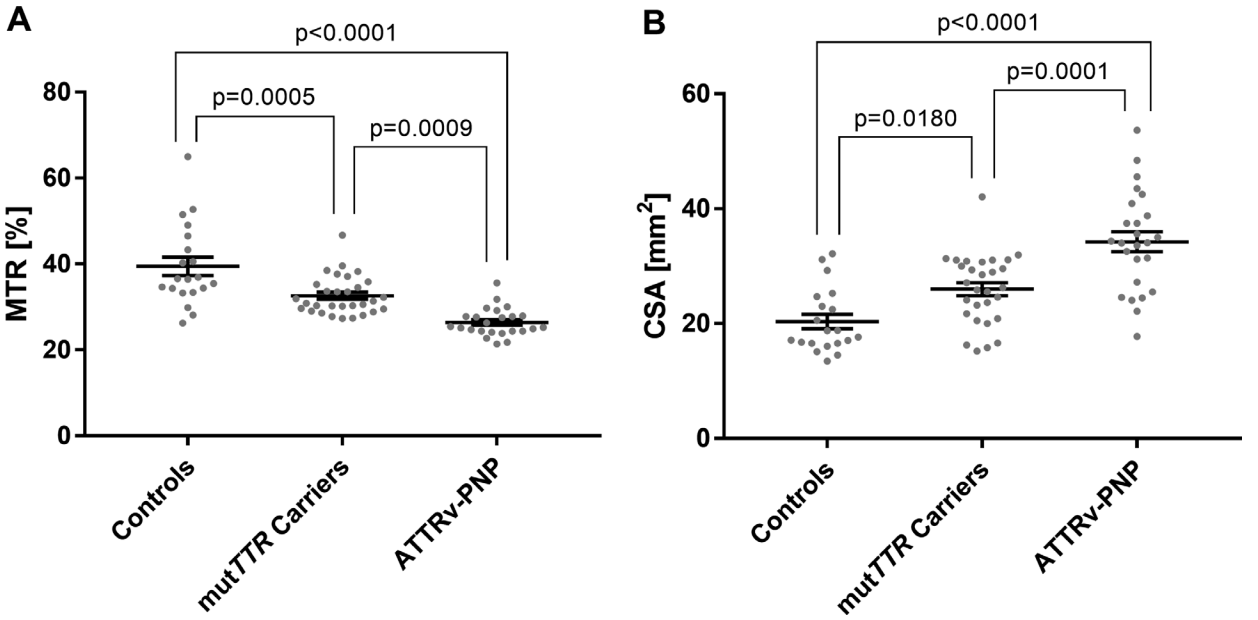

Figure 1. Quantitative MRN markers. Mean and individual values of sciatic nerve magnetization transfer ration (MTR; A) and cross sectional area (CSA; B) are plotted for controls, asymptomatic mut*TTR*-carriers, and symptomatic ATTRv-PNP patients. Sciatic nerve MTR was highest in healthy controls, decreased significantly in asymptomatic mut*TTR*-carriers, and even more in symptomatic ATTRv-PNP patients. Inversely, sciatic nerve CSA was significantly higher in asymptomatic mut*TTR*-carriers, and in symptomatic ATTRv-PNP patients. Note that individual MTR values in healthy controls showed a wider distribution than in asymptomatic mut*TTR*-carriers, and especially in symptomatic ATTRv-PNP patients. Contrariwise, individual CSA values presented with a wider distribution in asymptomatic mut*TTR*-carriers and even more in symptomatic ATTRv-PNP patients compared to healthy controls. Error bars represent SEM. Significant differences are indicated by *P*-values.

found in symptomatic ATTRv-PNP only. A correlation between peroneal nerve DMLs, peroneal and tibial CMAP amplitudes, and sural NCVs was not identifiable in asymptomatic mut*TTR*-carriers and symptomatic ATTRv-PNP. In addition, sciatic nerve CSA did not correlate with the NIS-LL.

Discussion

A rapidly progressive, distal-symmetric, axonal, sensorimotor PNP is one of the main manifestations in ATTRv amyloidosis and leads to a significant decline in patients' quality of life, affecting mobility, daily life activities, and the ability to work. Novel cost-intensive drug therapies were recently approved by the U.S. Food and Drug Administration (FDA) and the European Medicines Agency (EMA). Initial results were promising when therapy was started early, and showed a decrease or cessation of disease progression, and in some cases even an improvement of clinical symptoms.[4,5] Few studies suggest the potential use of serum or CSF neurofilaments as biomarkers in different neurologic disorders,[29–31] and one study indicates that plasma neurofilament light chain concentration is increased and correlates with the clinical severity in ATTRv-PNP.[32] However, there are still no proven biomarkers for (1) the early detection of nerve lesions that are not detectable by NCS, and (2) for the monitoring of peripheral nerve impairment under therapy. Recent studies suggest that the quantitative MRN parameter ρ might become the first imaging biomarker in ATTRv-PNP,[15,16] but the underlying macromolecular alterations leading to the observed increase of ρ remain unclear in ATTRv-PNP and in other diffuse neuropathies compared to controls.

Here, we report on the first study that applied MTC imaging in asymptomatic and symptomatic ATTRv-PNP. Our results demonstrate that the MTR of the sciatic nerve was highest in healthy controls, decreased in asymptomatic mut*TTR*-carriers, and decreased even more in patients with manifest ATTRv-PNP (Figs. 1A and 2), independent of the underlying *TTR* gene mutation. Moreover, we found a trend toward a lower MTR in severely affected ATTRv-PNP patients compared to patients with only mild to moderate PNP. Additional evaluation of sciatic nerve CSA confirmed findings from previous MRN studies in ATTRv-PNP,[15,16] in that nerve CSA increased in asymptomatic mut*TTR*-carriers and even more in manifest ATTRv-PNP compared to controls (Figs. 1B and 2).

MTC imaging is an MRI technique that is sensitive to protons bound to macromolecular structures, such as myelin lipids or collagen.[22] These bound protons have a very short T2 relaxation time preventing their signal to be

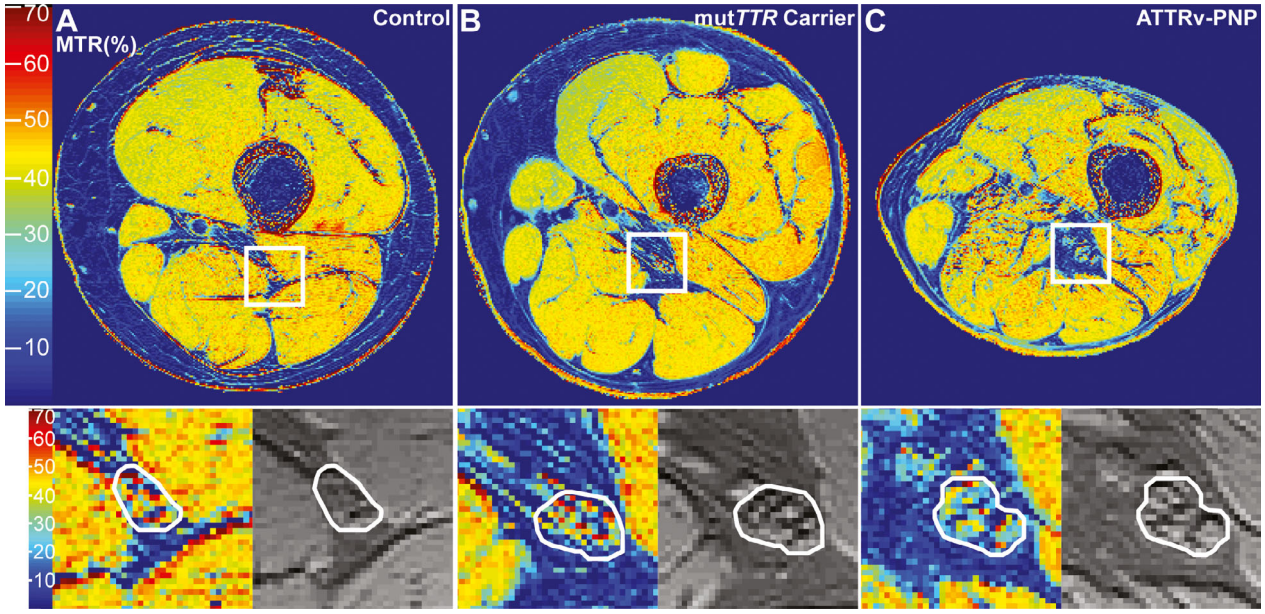

Figure 2. Magnetization transfer ratio map. Representative MTR pseudo-colorized (%) maps are shown for a healthy control (A), an asymptomatic mut*TTR*-carrier (B), and a symptomatic ATTRv-PNP patient (C). The white boxes in A–C are zoomed-in and displayed below to show detailed views of the MTR (%) map (left) and the MTC sequence without the off-resonance pulse (right) with the sciatic nerve encircled in white. Note the marked decrease of sciatic nerve MTR (%) in the asymptomatic mut*TTR*-carrier (loss of red and yellow signals), and even further decrease in the symptomatic ATTRv-PNP patient, compared to the control.

directly measured by conventional MRI sequences. MTC imaging overcomes this shortcoming by using an off-resonance pulse to saturate macromolecular bound protons. These saturated protons then exchange with free water protons and produce a decrease in signal intensity of the free water protons, allowing their visualization. This can be measured and quantified by computing the MTR.[33] Various MRI studies in demyelinating disorders of the central nervous system (CNS), including MS, demonstrated that changes of the MTR reflect the integrity of myelin structures and can thus be used for detecting and monitoring disease activity in MS patients.[34–37] Another histopathologic study focusing on axonal loss, investigated MS lesions as depicted by MRI in a large postmortem sample, and found a strong correlation between MTR and axonal density.[38] Furthermore, several longitudinal MTC imaging studies in MS proved that this technique can assist in estimating treatment effects on remyelination and protection against tissue damage in response to different immunosuppressive therapies.[39–44]

While results from these studies conducted in the CNS are promising, little is known about the potential of MTC imaging in the PNS. Findings from an experimental study investigating MTR characteristics of amphibian sciatic nerves in vitro at 3 Tesla magnetic field strength revealed that a change in MTR should not solely be regarded as an indicator for the degree of myelination, but should also consider axonal density.[23] Recent studies in healthy human volunteers proved that measuring the MTR in the median nerve and in foot nerves is feasible and directly applicable on standard clinical 3 Tesla MR scanners.[45–47] The first and hitherto sole clinical application study of MTC imaging in a peripheral neuropathy demonstrated a strong correlation between decreasing sciatic nerve MTR values and higher grades of disability in patients with demyelinating or axonal variants of Charcot–Marie–Tooth disease (CMT1A; CMT2A).[26]

Our results are in line with these findings and go beyond: a decrease in sciatic nerve MTR not only correlated with increasing clinical severity in ATTRv-PNP (as determined by the NIS-LL score; Table 1) but also differentiated between asymptomatic mut*TTR*-carriers and healthy controls, suggesting that a critical peripheral nerve damage precedes the symptomatic stage of the disease. By positively correlating with both, peroneal and tibial CMAP, and sural SNAP amplitudes in manifest ATTRv-PNP (Table 1), MTR reflects the extent of motor and sensory axonal degeneration. This is clinically relevant because MTR is still measurable and hence applicable for disease monitoring at more advanced PNP stages when neither CMAPs nor SNAPs are elicitable anymore. However, at this stage of the disease, patients can still be ambulant with or without assistance. Therewith, they are eligible and might benefit from one of the *TTR* knock-

down drugs, patisiran or inotersen, both being approved for ATTRv-PNP at familial amyloid polyneuropathy (FAP) stages 1 or 2, or from the TTR stabilizing drug tafamidis that, at least in Europe, is approved for FAP stage 1.[48]

ATTRv-PNP first manifests as small-fiber injury and then rapidly progresses by affecting larger, myelinated nerve fibers with a consecutive pathologic decrease of potentials in NCS, predominantly of sensory fibers. Early diagnosis of PNP and quick initiation of pharmacologic treatment is essential in the follow-up management of mut*TTR*-carriers as soon as they become clinically symptomatic. Here, MTR might be a helpful additional diagnostic tool that has high sensitivity for detecting very early PNP manifestations or even presymptomatic disease as sciatic nerve MTR positively correlated with sural SNAP amplitudes in our asymptomatic mut*TTR*-carrier cohort with consistently normal sural SNAPs.

A second clinically relevant scenario relates to the detection of disease progression during pharmacotherapy. At this stage of the disease, a selected therapy can still be switched, as at least one stage-dependent therapeutic alternative is available in case of progression. However, the established FAP stages according to Coutinho are above all geared to patient's ambulation.[48] Facing the variety of approved innovative pharmacotherapeutic options, this historic PNP stage classification is not anymore sensitive enough to objectify first signs of PNP progression on time. Therefore, novel biomarkers are needed to identify PNP progression under a given pharmacotherapy as timely and objectively as possible, that is, before it comes to a clinically relevant impairment of motor skills including ambulation. Future studies are required to test whether MTR can be further developed as a valid intraindividual marker that sensitively indicates PNP progression during therapy.

Unlike MTR, CSA (a MRN measure for nerve caliber) increased from healthy controls to mut*TTR*-carriers and further to ATTRv-PNP patients (Figs. 1B and 2) and correlated with electroneurographic parameters that are commonly ascribed to functions of the myelin sheath, that is, NCV and DML. In primary axonal PNPs such as in ATTRv-PNP, those NCS parameters do not become pathologic until a critical threshold of axonal injury is exceeded which is typically not the case at early disease stages. Moreover, a negative correlation of CSA with sural SNAPs was only given in symptomatic ATTRv-PNP, but not in asymptomatic mut*TTR*-carriers. Together with the finding that only the MTR correlated with the NIS-LL and thus with the clinical PNP stage, our data favor MTR to be a more promising imaging marker than CSA, even though both, MTR and CSA, can almost equally differentiate between healthy controls, asymptomatic mut*TTR*-carriers, and symptomatic ATTRv-PNP patients. Furthermore, a change in MTR represents a change in the macromolecular composition or rather in the pool of protons bound to macromolecules in nerve tissue, and is therewith more likely than CSA to early indicate a response or nonresponse to treatment when applied for therapeutic monitoring in the future.

This study is limited by a significant age difference between symptomatic ATTRv-PNP patients on the one hand (mean age 58.8 years), and asymptomatic mut*TTR*-carriers (mean age 43.3 years) and healthy controls (mean age 44.3 years) on the other. Due to the natural course of the disease, age differences between asymptomatic mut*TTR*-carriers and clinically symptomatic patients cannot be reasonably controlled as ATTRv-PNP manifests and progresses with increasing age. These age differences seem to be negligible due to an expected higher effect size in the symptomatic ATTRv-PNP group. In addition, confounding factors such as age, that have the potential to influence study results, are more likely to affect group comparisons between asymptomatic mut*TTR*-carriers and healthy controls than between symptomatic ATTRv-PNP and healthy controls. Therefore, we decided to match the age of our healthy controls with the age of the asymptomatic mut*TTR*-carriers. Restrictively, a previous study applying MTC imaging in healthy controls showed a potential effect of age on sciatic nerve MTR with an age-dependent MTR decrease.[25] Even though we cannot fully exclude that the older age in our manifest ATTRv-PNP patients mildly amplified the observed MTR decrease, one has to consider that in the mentioned control study i) age differences averaged 32.5 years and were therewith much higher than the age differences in our study (approximately 15 years), and ii) most importantly, age differences were not observable when evaluating the sciatic nerve MTR at either proximal or distal thigh positions only.[25]

Previous MRN work proved that the peripheral nerve lesion pattern observed in ATTRv-PNP is non-diffuse and that the thigh level is the site of predominant nerve injury.[15] Furthermore, the MTR of intact lower extremity nerves does not show a proximal-to-distal gradient so that referencing MTR values for anatomical nerve location is not required.[25] Both facts contribute to a short MRI protocol with a reasonable total acquisition time which can be easily integrated into routine clinical follow-up examinations. However, further rigorous studies are needed to determine the future role of MRN in the clinical management of ATTRv-PNP patients and asymptomatic mut*TTR*-carriers.

In conclusion, this study shows that (i) MTC imaging of the sciatic nerve at the thigh level is clinically feasible,

(ii) MTR can be used to quantify macromolecular changes in ATTRv-PNP, and iii) MTR differentiates between symptomatic ATTRv-PNP and asymptomatic mut*TTR*-carriers with high sensitivity while correlating well with electrophysiologic examination results, and the NIS-LL. To prove the validity of MTR as a robust imaging biomarker in comparison with the other two recently established quantitative MRN markers, $T2_{app}$ and especially ρ, intraindividual longitudinal comparisons are needed and are already subject of ongoing investigations. With its ability to give an inside view into nerve tissue integrity in vivo, MTC imaging might then help to better monitor both, ATTRv-PNP patients on causative pharmacotherapies, and asymptomatic mut*TTR*-carriers.

Acknowledgments

The study was supported in part by Alnylam Pharmaceuticals (research grant to J.K.), the Medical Faculty of the University of Heidelberg (Olympia Morata stipend grant to J.K.), and the German Research Foundation (SFB 1118 to S.H., SFB 1158 to M.B.). S.H. was supported by the Dietmar Hopp Foundation, and M.B. by Siemens Healthcare, the Dietmar Hopp Foundation, and the European Union (Horizon 2020). The authors thank Dorothea Willich (Department of Neuroradiology, Heidelberg University Hospital) for her ongoing support and excellent technical performance of all MRN examinations.

Conflict of Interest

J. Kollmer received a research grant and lecture honoraria from, and E. Hund and M. Weiler advise for Alnylam Pharmaceuticals that owns patent rights to Patisiran (Onpattro®), a drug that was mentioned in this study. J. Kollmer, E. Hund, and M. Weiler advise for and/or received lecture honoraria from Akcea Therapeutics that owns patent rights to Inotersen (Tegsedi®), a drug that was mentioned in this study. J. Kollmer, U. Hegenbart, E. Hund, J. Purrucker, and M. Weiler advise for and/or received financial support for conference attendance, and lecture honoraria from Pfizer that owns patent rights to Tafamidis (Vyndaqel®), a drug that was mentioned in this study.

Author Contributions

J.K., U.H., S.H., and M.W. conceived and designed the study. Acquisition and analysis of data were accomplished by J.K., U.H., C.K., E.H., J.C.P., J.M.H, S.I.L, G.S., S.O.S., J.M.E.J., S.H., and M.W. J.K., U.H., J.M.H., S.I.L., S.O.S., M.B., S.H., and M.W. were responsible for writing and drafting a significant portion of the manuscript or figures.

References

1. Hund E, Linke RP, Willig F, Grau A. Transthyretin-associated neuropathic amyloidosis: pathogenesis and treatment. Neurology 2001;56:431–435.
2. Plante-Bordeneuve V, Lalu T, Misrahi M, et al. Genotypic-phenotypic variations in a series of 65 patients with familial amyloid polyneuropathy. Neurology 1998;51:708–714.
3. Coelho T, Maia LF, Martins da Silva A, et al. Tafamidis for transthyretin familial amyloid polyneuropathy: a randomized, controlled trial. Neurology 2012;79:785–792.
4. Adams D, Gonzalez-Duarte A, O'Riordan WD, et al. Patisiran, an RNAi therapeutic, for hereditary transthyretin amyloidosis. N Engl J Med 2018;379:11–21.
5. Benson MD, Waddington-Cruz M, Berk JL, et al. Inotersen treatment for patients with hereditary transthyretin amyloidosis. N Engl J Med 2018;379:22–31.
6. Thomas PK, King RH. Peripheral nerve changes in amyloid neuropathy. Brain 1974;97:395–406.
7. Said G, Ropert A, Faux N. Length-dependent degeneration of fibers in Portuguese amyloid polyneuropathy: a clinicopathologic study. Neurology 1984;34:1025–1032.
8. Plante-Bordeneuve V, Said G. Familial amyloid polyneuropathy. Lancet Neurol 2011;10:1086–1097.
9. Adams D, Cauquil C, Labeyrie C. Familial amyloid polyneuropathy. Curr Opin Neurol 2017;30:481–489.
10. Plante-Bordeneuve V, Ferreira A, Lalu T, et al. Diagnostic pitfalls in sporadic transthyretin familial amyloid polyneuropathy (TTR-FAP). Neurology 2007;69:693–698.
11. Bendszus M, Stoll G. Technology insight: visualizing peripheral nerve injury using MRI. Nat Clin Pract Neurol 2005;1:45–53.
12. Kollmer J, Bendszus M, Pham M. MR neurography: diagnostic imaging in the PNS. Clin Neuroradiol 2015;25 (Suppl 2):283–289.
13. Pham M, Baumer P, Meinck HM, et al. Anterior interosseous nerve syndrome: fascicular motor lesions of median nerve trunk. Neurology 2014;82:598–606.
14. Jende JME, Hauck GH, Diem R, et al. Peripheral nerve involvement in multiple sclerosis: demonstration by magnetic resonance neurography. Ann Neurol 2017;82:676–685.
15. Kollmer J, Hund E, Hornung B, et al. In vivo detection of nerve injury in familial amyloid polyneuropathy by magnetic resonance neurography. Brain 2015;138:549–562.
16. Kollmer J, Sahm F, Hegenbart U, et al. Sural nerve injury in familial amyloid polyneuropathy: MR neurography vs clinicopathologic tools. Neurology 2017;89:475–484.
17. Kollmer J, Weiler M, Purrucker J, et al. MR neurography biomarkers to characterize peripheral neuropathy in AL amyloidosis. Neurology 2018;91:e625–e634.
18. Pham M, Oikonomou D, Hornung B, et al. Magnetic resonance neurography detects diabetic neuropathy early and with Proximal Predominance. Ann Neurol 2015;78:939–948.

19. Kronlage M, Baumer P, Pitarokoili K, et al. Large coverage MR neurography in CIDP: diagnostic accuracy and electrophysiological correlation. J Neurol 2017;264:1434–1443.
20. Kronlage M, Knop KC, Schwarz D, et al. Amyotrophic lateral sclerosis versus multifocal motor neuropathy: utility of MR neurography. Radiology 2019;292:149–156.
21. Kollmer J, Preisser P, Bendszus M, Kele H. Fascicular torsions of the anterior and posterior interosseous nerve in 4 cases: neuroimaging methods to improve diagnosis. J Neurosurg 2019. Epub ahead of print. https://doi.org/10.3171/2019.3.JNS183302
22. Wolff SD, Balaban RS. Magnetization transfer contrast (MTC) and tissue water proton relaxation in vivo. Magn Reson Med 1989;10:135–144.
23. Does MD, Beaulieu C, Allen PS, Snyder RE. Multi-component T1 relaxation and magnetisation transfer in peripheral nerve. Magn Reson Imaging 1998;16:1033–1041.
24. Henkelman RM, Stanisz GJ, Graham SJ. Magnetization transfer in MRI: a review. NMR Biomed 2001;14:57–64.
25. Kollmer J, Kastel T, Jende JME, et al. Magnetization transfer ratio in peripheral nerve tissue: does It depend on age or location? Invest Radiol 2018;53:397–402.
26. Dortch RD, Dethrage LM, Gore JC, et al. Proximal nerve magnetization transfer MRI relates to disability in Charcot-Marie-Tooth diseases. Neurology 2014;83:1545–1553.
27. Bril V. NIS-LL: the primary measurement scale for clinical trial endpoints in diabetic peripheral neuropathy. Eur Neurol 1999;41(Suppl 1):8–13.
28. Cabana JFGY, Boudreau M, Levesque IR, et al. Quantitative magnetization transfer imaging made easy with qMTLab: software for data simulation, analysis, and visualization. Concepts Magn Reson 2016;44A:263–277.
29. Khalil M, Teunissen CE, Otto M, et al. Neurofilaments as biomarkers in neurological disorders. Nat Rev Neurol 2018;14:577–589.
30. Poesen K, De Schaepdryver M, Stubendorff B, et al. Neurofilament markers for ALS correlate with extent of upper and lower motor neuron disease. Neurology 2017;88:2302–2309.
31. Disanto G, Barro C, Benkert P, et al. Serum neurofilament light: a biomarker of neuronal damage in multiple sclerosis. Ann Neurol 2017;81:857–870.
32. Kapoor M, Foiani M, Heslegrave A, et al. Plasma neurofilament light chain concentration is increased and correlates with the severity of neuropathy in hereditary transthyretin amyloidosis. J Peripher Nerv Syst 2019;24:314–319.
33. McGowan JC. The physical basis of magnetization transfer imaging. Neurology 1999;53:S3–S7.
34. Brochet B, Dousset V. Pathological correlates of magnetization transfer imaging abnormalities in animal models and humans with multiple sclerosis. Neurology 1999;53:S12–S17.
35. Richert ND, Frank JA. Magnetization transfer imaging to monitor clinical trials in multiple sclerosis. Neurology 1999;53:29–32.
36. van Waesberghe JH, Barkhof F. Magnetization transfer imaging of the spinal cord and the optic nerve in patients with multiple sclerosis. Neurology 1999;53:46–48.
37. De Stefano N, Battaglini M, Stromillo ML, et al. Brain damage as detected by magnetization transfer imaging is less pronounced in benign than in early relapsing multiple sclerosis. Brain 2006;129:2008–2016.
38. van Waesberghe JH, Kamphorst W, De Groot CJ, et al. Axonal loss in multiple sclerosis lesions: magnetic resonance imaging insights into substrates of disability. Ann Neurol 1999;46:747–754.
39. Chen JT, Collins DL, Atkins HL, et al. Magnetization transfer ratio evolution with demyelination and remyelination in multiple sclerosis lesions. Ann Neurol 2008;63:254–262.
40. Zivadinov R, Dwyer MG, Hussein S, et al. Voxel-wise magnetization transfer imaging study of effects of natalizumab and IFNbeta-1a in multiple sclerosis. Mult Scler 2012;18:1125–1134.
41. Button T, Altmann D, Tozer D, et al. Magnetization transfer imaging in multiple sclerosis treated with alemtuzumab. Mult Scler 2013;19:241–244.
42. Brown RA, Narayanan S, Arnold DL. Segmentation of magnetization transfer ratio lesions for longitudinal analysis of demyelination and remyelination in multiple sclerosis. NeuroImage 2013;66:103–109.
43. Zivadinov R, Dwyer MG, Markovic-Plese S, et al. Effect of treatment with interferon beta-1a on changes in voxel-wise magnetization transfer ratio in normal appearing brain tissue and lesions of patients with relapsing-remitting multiple sclerosis: a 24-week, controlled pilot study. PLoS One 2014;9:e91098.
44. Arnold DL, Gold R, Kappos L, et al. Magnetization transfer ratio in the delayed-release dimethyl fumarate DEFINE study. J Neurol 2014;261:2429–2437.
45. Gambarota G, Mekle R, Mlynarik V, Krueger G. NMR properties of human median nerve at 3 T: proton density, T1, T2, and magnetization transfer. J Magn Reson Imaging 2009;29:982–986.
46. Gambarota G, Krueger G, Theumann N, Mekle R. Magnetic resonance imaging of peripheral nerves: differences in magnetization transfer. Muscle Nerve 2012;45:13–17.
47. Mekle R, Mortamet B, Granziera C, et al. Magnetization transfer-based 3D visualization of foot peripheral nerves. J Magn Reson Imaging 2013;37:1234–1237.
48. Coutinho P, Martins da Silva A, Kopes Lima J, Resende Barbosa A. Forty years of experience with type 1 amyloid neuropathy. Review of 483 cases. In: Glenner GG, Pinhoe Costa P, Folcao de Freitas A, eds. Amyloid and Amyloidosis. Amsterdam: Excerpta Medica, 1980.

